九州大学学術情報リポジトリ
Kyushu University Institutional Repository

Development and Testing of a High Performance Airfoil for Application in Small Horizontal Axis Wind Turbine Blades

Manoj Kumar Chaudhary
Department of Mechanical Engineering, Trinity Academy of Engineering

Shrivastava, Akash
TSSM's Padmabhooshan Vasantdada Patil Institute of Technology

Sandeep S. Kore
Vishwakarma Institute of Information Technology

RajuSing D. Rathod
K. J. College of Engineering and Management Research

他

https://doi.org/10.5109/7172280

出版情報：Evergreen. 11 (1), pp.275-285, 2024-03. Interdisciplinary Graduate School of Engineering Sciences, Kyushu University, Japan
バージョン：
権利関係：Creative Commons Attribution 4.0 International

KYUSHU UNIVERSITY

Development and Testing of a High Performance Airfoil for Application in Small Horizontal Axis Wind Turbine Blades

Manoj Kumar Chaudhary[1], Akash Shrivastava[2], Sandeep S. Kore[3], RajuSing D. Rathod[4], Nikhil R. Kadam[5], K. B. Gavali[6]

[1,6]Department of Mechanical Engineering, Trinity Academy of Engineering, Pune, India

[2]TSSM's Padmabhooshan Vasantdada Patil Institute of Technology, Pune, India

[3]Vishwakarma Institute of Information Technology, Pune, India

[5]School of Mechanical and Manufacturing, Sciences, JSPM University, Pune, India

[4]K. J. College of Engineering and Management Research, Pune, India

*Author to whom correspondence should be addressed:
E-mail: manojzf2011@gmail.com

(Received July 28, 2023: Revised December 03, 2023: Accepted January 16, 2024).

Abstract: The low aerodynamic airfoil performance is a common challenge. This research project used the X-Foil program to generate three high aerodynamic performances (MKC-Series) airfoil. These airfoil were optimized for SHAWT blades with a Rekynolds number ranging from 100,000 to 300,000. An application in Matlab was developed using blade geometry optimization and BEM theory. Using new airfoil (MKC series), an optimal design technique based on BEM Theory is investigated when applied to the blade geometry of wind turbine rotors with a 0.2 m radius. Wind turbine rotor blades refined through experimentation were made using additive manufacturing utilizing 3D printing. Lower wind speeds were found to be more suitable for the MKC-Series airfoil than for the SG6043 airfoil.

Keywords: BEMT; HAWT; VAWT; CFD; TSR.

1. Introduction

Energy is fundamental to social and economic development, and it plays a major role in the environments in which people live and work. The use of wind energy, a sustainable energy source, is growing in technology applications. The improved HAWT blade design geometry can be utilized next to highways or atop buildings since it can lower initial speed without the need for an external push[1–3]. An evaluation of the differences between optimizing the distribution with enhanced blade geometry of blades [4-5]. An examined into methods to increase modest wind turbines' yearly energy output. The curvature radius and cant angle of winglets have an impact on blade performances. [6–10]. The blade design of TSR of a 2 kW HAWT was optimized. BEMT theory has been presented to correlate the blade geometry of constant chord untwisted turbines[11–13]. There are specific airfoil designed to be used in low wind conditions. Gigueŕe and Selig developed investigated the effects along the blades of thin airfoil from the SG60XX series which are appropriate for application of HAWT Blade at low Reynolds number. Enhancing the wind turbine's output and the aerodynamic characteristics of its blade vortices is one method to reduce lift force and enhance drag. Multiple dimensions of optimization should be applied to the small wind turbine blades. These designs offer a multitude of design options for blades for various applications, like quiet blades for building mounting or quick-start blades for low wind settings.[14–16]. For SWAT, airflows with Reynolds numbers (Re) less than 500,000 are frequently employed to characterize low wind speeds. The free source X-Foil, Cura software was used to optimize the HAWT blade utilizing a BEM technique. Few studies have looked at the optimization and experimentation of the aerodynamic performance of airfoil and 3D printed wind turbine blades, according to the previously mentioned literature analysis [17–18]. In this work, the 0.4 m diameter, three-bladed, horizontal axis wind turbine rotor is designed and operationally evaluated for Re=10,00,00 to 30,00,00 applications. The NAF series airfoil were researched and developed for application in small HAWT rotors at low Re and low wind speeds. Utilizing 3D printers, 3-bladed small wind turbine rotors with high L/D and Maximum Cl were created for the MKC-Series airfoil parametric investigation revealed that the blade geometry with the optimal blade geometry. Maximum power coefficient CP values of 0.46, 0.5, and 0.48 were achieved with a (3, 5, and 7 bladed) rotor at the tip speed ratios of 7, 5, and 4. A BEM-theory based computation code is used to optimise HAWT blades. At approximately 6 m/s, the maximum power coefficient

value (0.371 for the tested rotor and 0.388 for the optimised rotor) is attained.

The wind power produced by the exhaust from air conditioners has been employed as a wind energy source to produce electrical energy[19-23]. The CFD software tool is used to calculate the thermal effects on blade. Energy sources like solar energy and wind energy, which are already well-known, are the focus of many research efforts[24-25]. In order to analyze the vertical axis wind turbine (VAWT) blade thickness was varied using the ANSYS Fluent program. Wind energy and other renewable energy sources are predicted to increase potentially during the next ten years[26-28]. The highest power coefficient exhibits a 40% performance improvement in the modified model. It is possible to boost the turbine Cp by up to 1.23 times in order to make up for the poor efficiency and shortage of Savonius turbines. Numerically a turbine performance with a conventional and an elliptical blade was investigated[29-31]. The 3-bladed rotors power at various wind speeds and blade pitch angles in order to carry out the experimental research.

Airfoil and 3D printed wind turbine blade aerodynamic performance is optimized and tested using the thickness-to-camber ratio (t/c). Results of a three-bladed, 0.4-meter-diameter tiny horizontal axis wind turbine rotor created The main objective of this project is to analyze existing airfoils and create high-performance airfoils that may be employed in small wind turbines at low Reynolds numbers. The subsequent illustrations will help simplify this paper's objectives such as Examine the MKC-series and SG 6043 airfoils' aerodynamic performance (from 10,00,00 to 30,00,00 Reynolds numbers). the creation of three Based on the ideal t/c, a new airfoil creation of a novel airfoil and an improved wind turbine blade via prototype methods Using X-Foil software, novel airfoil research is numerically simulated.

2. Design methodology

2.1 Design and optimization of a low Reynolds number airfoil through X-Foil.

However, X-Foil software was used to simulate and analyze a number of low-wind HAWT airfoil that are currently in use. A new airfoil (MKC Series). To examine the aerodynamic properties for the purpose of designing and optimizing new airfoil, 251 coordinate points were considered in this instance using the X-Foil software. The AF1, AF2 and AF3 airfoil were followed by the creation of three further airfoil. The SG6043 airfoil and these new airfoil aerodynamic performance are compared in Sections 3 and 4.

3D printing was used to manufacture the hub and blade. The 3-blade rotor was manufactured using PLA material to reduce weight.

In this research work are introduction presented in the section 1. The small wind turbine geometry optimization method is presented in Section 2. The blade and airfoil simulation analytical simulation is presented in Section 3. The production and product design of small wind turbine is presented in Section 4. The findings of blade configuration, TSR ratio, solidity, and the use of new airfoil along the same edge is presented in Section 5. MKC 7-6, MKC8-6 and MKC9-6 is designated as New Airfoil Series NAF1, NAF2 & NAF3 respectively.

2.2 Airfoil design and optimization

X-Foil and Matlab software were used to test a range of HAWT airfoil. Based on t/c ratio, the greatest lift-to-drag ratio and highest lift coefficient at Re (Reynolds Number) varied from 100,000 to 300,000. In Fig 1, these variances are displayed. it was found that the aerodynamic performance improved with increasing values of Re. this study's t/c range was 0.8 to 1.5. The XFOIL software results showed that thicknesses of 7%, 8%, and 9% and camber of 6% were the optimal zones for designing a new airfoil with the highest possible aerodynamic properties., the t/c range is 0.8-1.50. Three airfoil have been built in this zone using the codes NAF1, NAF2, and NAF3. Table 1 shows the specifications for thickness and camber. Figure. 1 summarizes the optimization and analysis of the airfoil.

Figure. 2 displays the new airfoil geometrical properties and profiles.

A number of existing low wind speed HAWT airfoil were optimized using X-Foil. Fig. 2, shows the new airfoil that were created using the X-Foil software. Based on t/c ratios ranging from 10,00,00 to 30,00,00.

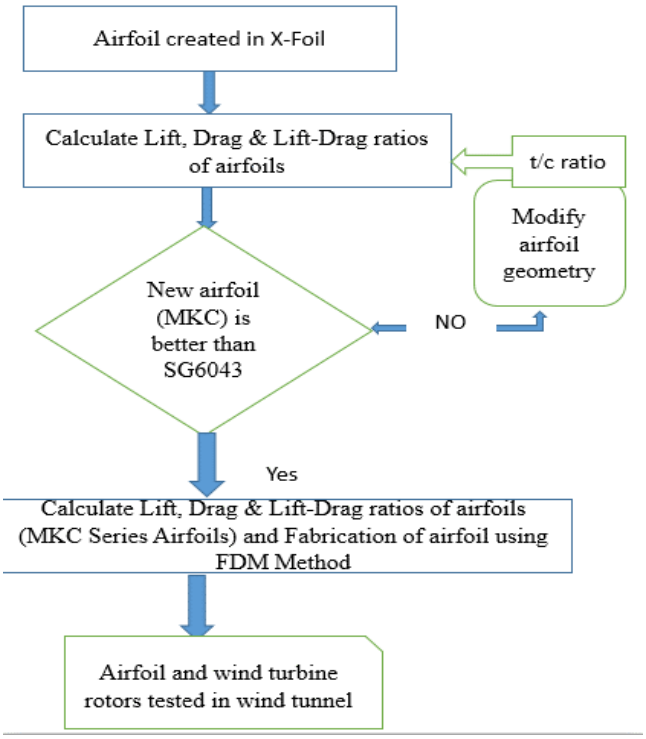

Fig. 1: An overview of the XFOIL process for designing and testing airfoil in wind tunnels

Equations (1) and (2) were used to compute the lift (CL) and drag (CD), respectively.

$$C_L = \frac{L}{\frac{1}{2}\rho V_\infty^{\,2} A} \quad (1)$$

$$C_D = \frac{D}{\frac{1}{2}\rho V_\infty^{\,2} A} \quad (2)$$

Table 1. Optimizing camber quantities and thickness for SG6043 and NAF-Series airfoil

Airfoil	Thickness (% c)	Camber (% c)
SG6043	10.01	5.5
NAF1	7	6
NAF2	8	6
NAF3	9	6

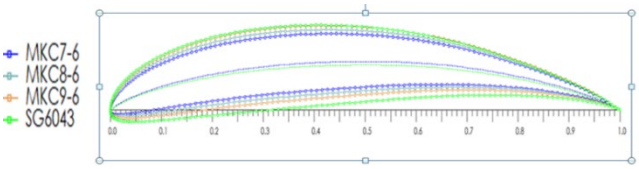

Fig. 2: Developed 2D-airfoil (MKC Series & SG6043)

2.3 Comparison of the base (SG6043) and MKC-Series airfoil for small wind turbines operating at low Reynolds numbers.

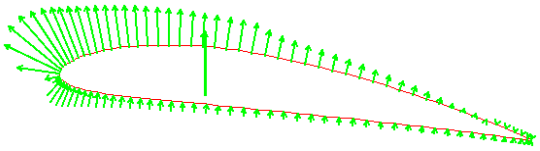

Fig. 3: New airfoil pressure curve at AOA=8°

Figures 3 and 4 display the pressure curve and 2D model of the modified airfoil at an optimal angle of attack of 8 degrees. An airfoil model made with Cura software is displayed in Fig. 5.

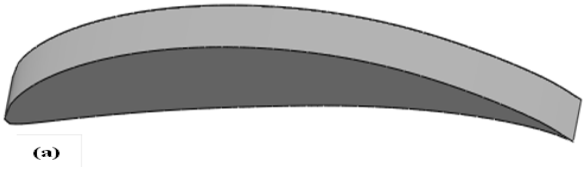

Fig 4: 2D-airfoil model Airfoil model in XFOIL software

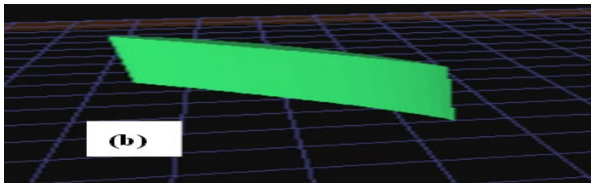

Fig. 5: 2D-airfoil model Airfoil model in Cura software

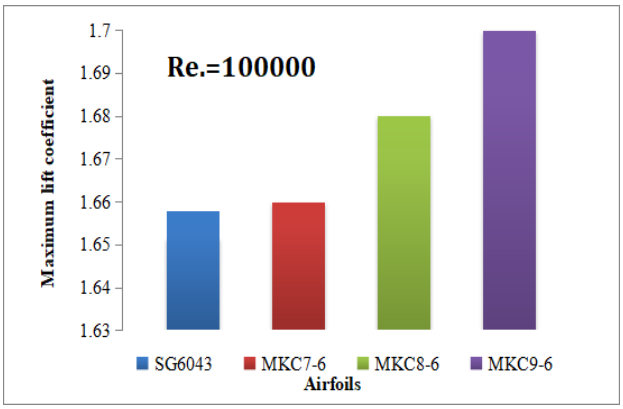

(a)

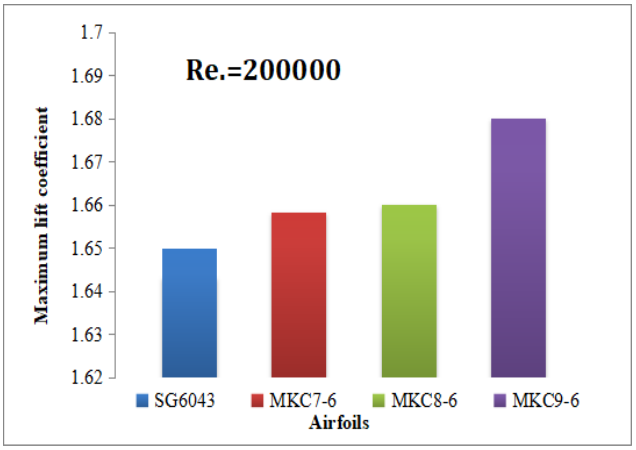

(b)

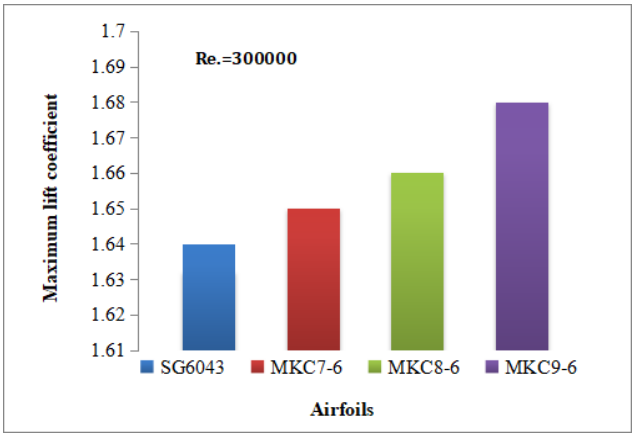

(c)

Fig. 6: Maximum lift coefficient of SG6043 and MKC-Series airfoil at various Regarding (a) (b) Re=100000 (c) Re= 200000 (c) Re= 300000.

2.4 Analysis of airfoil and fabrications

With a t/c range of 0.8 to 1.6, the airfoil was numerically analysed and optimized using X-Foil and Cura 4.1.0. Fig. 7 depicts a horizontal axis wind turbine. Figures 4 and 5 display the research and built model of the SG6043 and MKC-Series airfoil at Re=100,000. Four airfoil were produced using a 3D printer and PLA material.

Every airfoil has a camber of 6% c, a span length of 0.02 m, and a blade length of 0.05 m. The trailing edges of the MKC-Series airfoil are the roughest when compared to the basic airfoil. The construction of the airfoil took about 160 minutes. The machining parameter for an airfoil was optimized using cero software. Figure 8(a) displays the results of the airfoil studies. Displayed are the final printed MKC-Series and the base airfoil. Fig. 8(b).

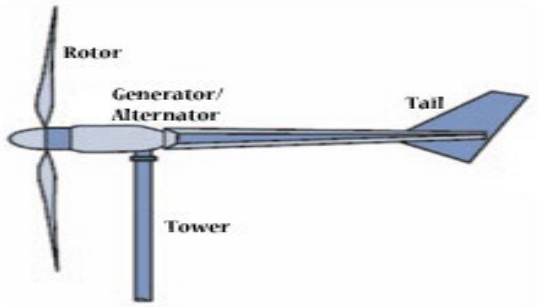

Fig. 7: Horizontal axis wind turbine (HAWT)

Fig. 8: 3D-simulation and model of new airfoil

Table 2. Design parameters simulation details

Parameters	Descriptions
Blade pitch angle	0º to 90º
Blade Number (B)	3, 4, 5, 6 & 7
Angle of attack (α)	2º to 20º
Tip speed ratio (λ)	2 to 8
Solidity (σ)	0.057 to 0.287

The design variable parameters are tabulated in Table 2.

3. Fabrications and Experimentation work

3.1 Fabrication of small wind turbine rotor blade

Optimized horizontal axis wind turbine blade structures are shown in Table 2 & Table 3, after printing PLA filaments at 205 °C for the nozzle, 60 °C for the bed, and 50 mm/s for print speed. The blade's fabrication using the MKC9-6 airfoil is depicted in Fig. 9. In order to increase aerodynamic performance, the suggested airfoil blade model was imported into the X-Foil program and given a round tip, as shown in Fig 9(b). The diameter of the rotor is 0.4 m.

Table 3. Specifics of the data on optimal blade geometry

Position	Chord, c (m)	Twist angle(deg.)	Airfoil
0	0.012	0	Circular
0.015	0.012	0	Circular
0.02	0.012	0	Circular
0.05	0.042	19.45	MKC9-6
0.072	0.035	14.31	MKC9-6
0.088	0.029	10.85	MKC9-6
0.104	0.026	8.33	MKC9-6
0.12	0.0221	6.52	MKC9-6
0.136	0.01969	5.08	MKC9-6
0.152	0.018	3.94	MKC9-6
0.168	0.016	3.015	MKC9-6
0.184	0.015	2.24	MKC9-6
0.196	0.014	1.59	MKC9-6
0.2	0.002	0	Circular

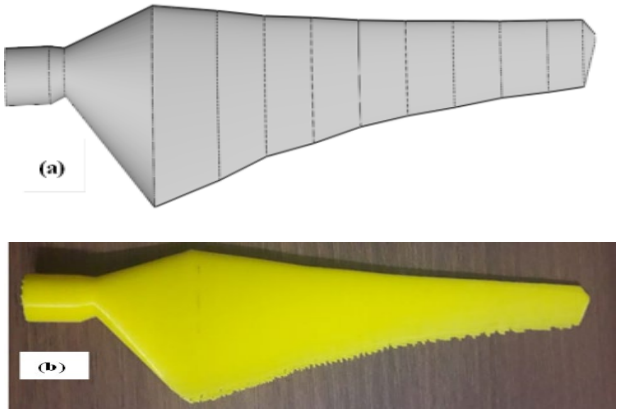

Fig. 9: Optimized blade model of MKC series airfoil (a) 2D-model in X-Foil (b) 3D printed blade

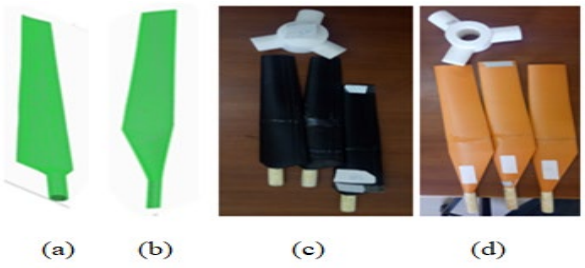

Fig. 10: Optimized Blade model with different blade length.

3D-dimensional and 3D-printed optimized rotor radius of 0.2 m and 0.4 m is shown in Fig. 10.

3.2 Experimental Investigation

The results of tests on the suggested airfoil carried out at various AOAs and wind speeds inside the test section are displayed in Fig. 11.

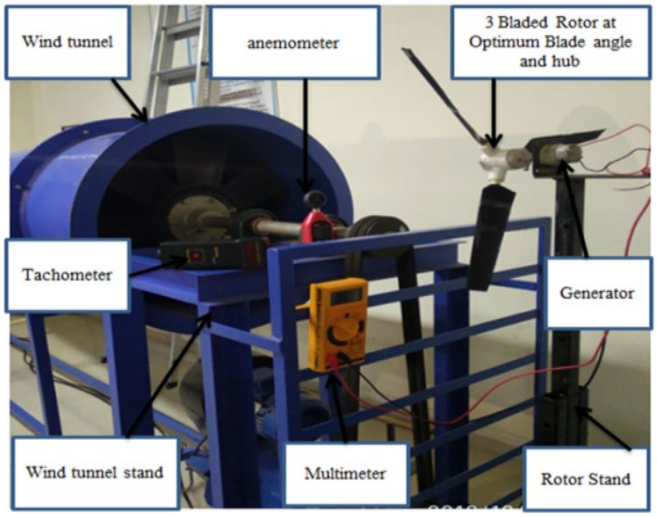

Fig. 11: Experimental setup

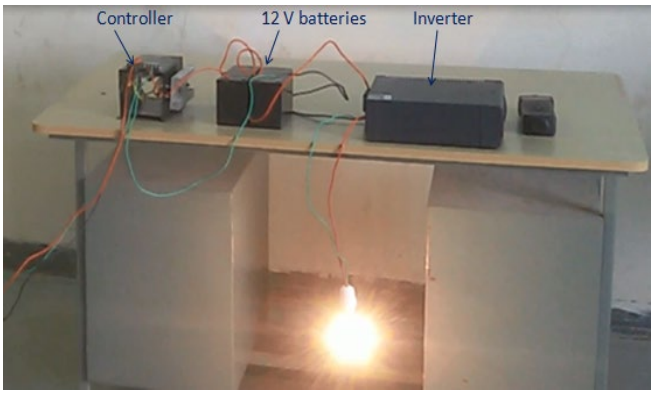

Fig. 12: Inverter battery setup

Figure 11., shows a schematic configure ation of a 0.2 m rotor radius with 3-bladed testing in a wind tunnel. Fig.12, explains how to set up an inverter battery system for voltage and current calculations.
A test segment of 0.3 m × 0.3 m × 1 m is available in the wind tunnel.

Fig. 13: New Airfoil model (NAF & SG6043)The rotor blade and airfoil model are printed using PLA and ABS filaments, respectively, and are constructed of wood.

3.3 Rotor Specification:

Hub diameter: 0.4 m, diameter: 0.024 m The twist angles at the root and tip are 1.59 and 19.45 degrees, respectively. The chord lengths are 0.042 meters at the root and 0.014 meters at the tip, respectively. Attack angle: 4.5°, tip speed ratio: 5.5 Solidity of the rotor: 5.49% Section of the MKC9-6 airfoil Six meters per second is the listed wind speed, and a PLA blade composition was chosen. The FDM procedure is used in the fabrication method. The optimized blade tip was designed to have a circular airfoil with a radius of 0.02 m. The airfoil model for rotor testing and blade manufacturing is shown in Fig. 13. The blades are fixed into the hub. Four distinct pitch angles were used to measure the turbine's electrical power output: 0°, 15°, 30°, and 45°. A rotor pitch angle of 30 degrees is suitable for performance analysis at wind speeds ranging from 3 to 6 m/s.

4. Results and Discussions

4.1 Lift performance of NAF airfoil and SG6043 base airfoil

Figure 14(a-c), shows the lift coefficient performance curves for the MKC-Series and SG6043 airfoil at Re=100,000 to 300,000. Using the X Foil software, the basic SG6043 and NAF-Series airfoil is analyzed by varying the AOA from 0º to 15º and Re from 100,000 to 300,000. The results of the study indicate that the lift coefficients of the NAF1, NAF2, NAF3, and SG6043 airfoil at Re=200,000 are 1.63, 1.66, 1.67, and 1.65 at AOAs of 13°, 14°, 16°, and 15°, respectively. The airfoil NAF1, NAF2 NAF3 and SG6043. The numerical results of the NAF3 airfoil drag performance when Re is varied from 100,000 to 300,000 are displayed in Fig. 14(d).
The simulation findings show that for AOAs of 6º, 12º, and 15º at Re=300,000. It has also been shown that the drag coefficient reduced as the Reynolds number climbed Re goes up from 10,00,00 to 30,00,00, and Cd goes down by about 5% to 15%

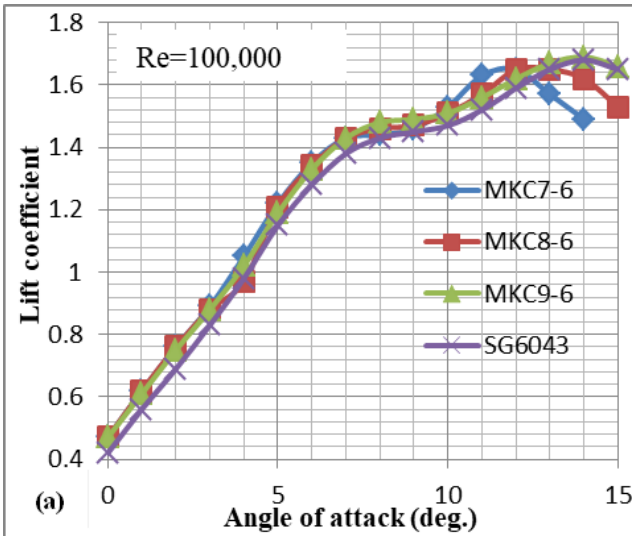

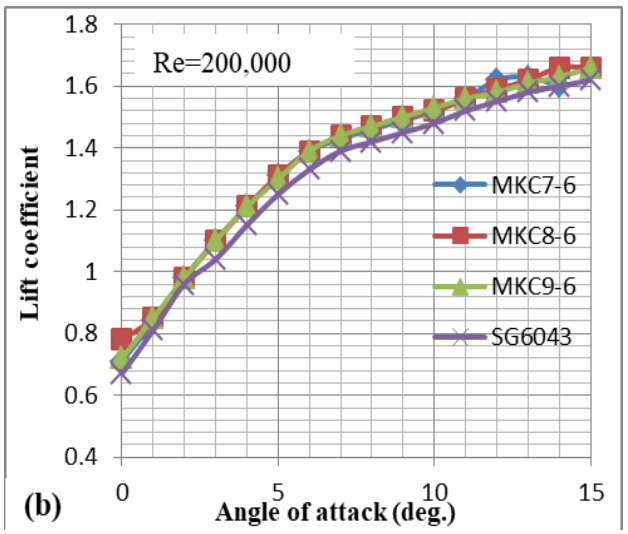

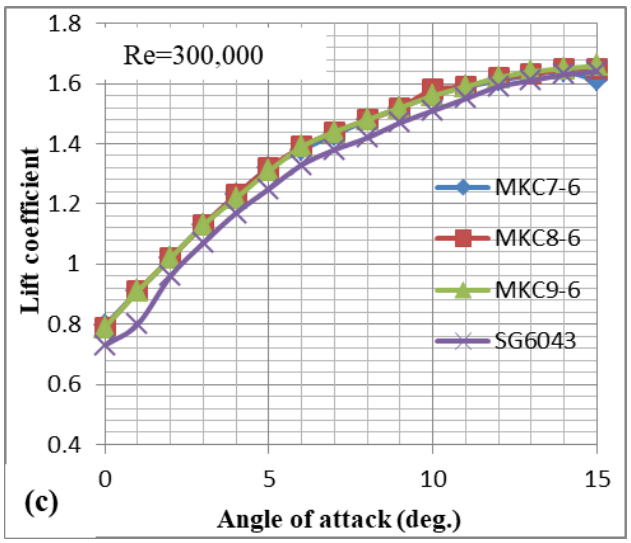

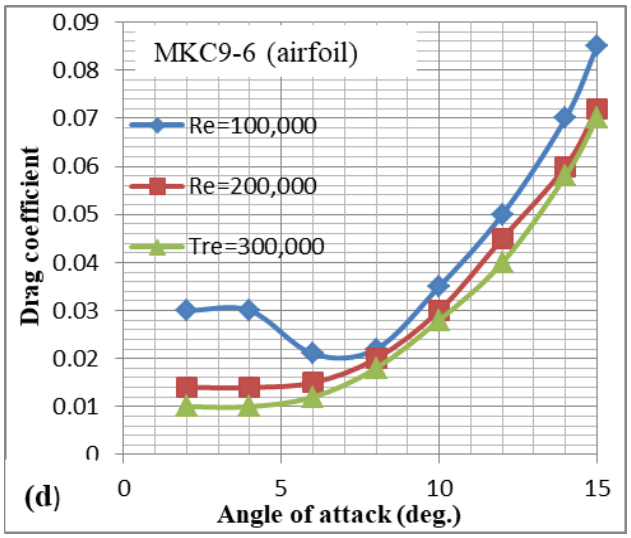

Fig. 14: Lift and drag performance versus AOA of SG6043 and MKC-series airfoil (a) Re=100,000 (b) Re=100,000 (c) Re=300,000 (d) MKC9-6 airfoil at Re=100,000 to 300,000

4.2 Lift –to- drag ratio of MKC-Series airfoil and SG6043 base airfoil

Table 4. Lift and drag coefficient results for new airfoil

AOA (°)	Lift Coefficient	Drag Coefficient
0	0.6890	0.0157
2	0.9715	0.0185
4	1.1950	0.0222
6	1.3665	0.0325
8	1.4687	0.0407
10	1.4240	0.0547

Table 5. Lift and drag coefficient results for SG6043 airfoil

AOA (°)	Lift Coefficient	Drag Coefficient
0	0.7324	0.0215
2	0.9437	0.0233
4	1.1380	0.0124
6	1.2936	0.0337
8	1.3740	0.0419
10	1.3512	0.0570

The findings of the new airfoil and the baseline model (SG6043) are displayed in Tables 4 and 5 together with the coefficient of lift and drag values at different angles of attack. An excellent agreement is found when comparing the CFD findings of aerodynamic values with the X-Foil results.

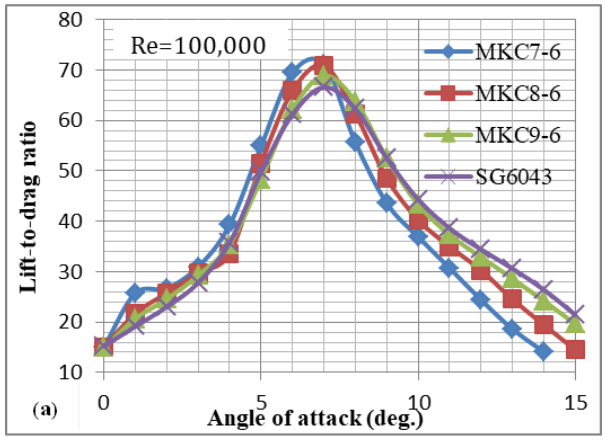

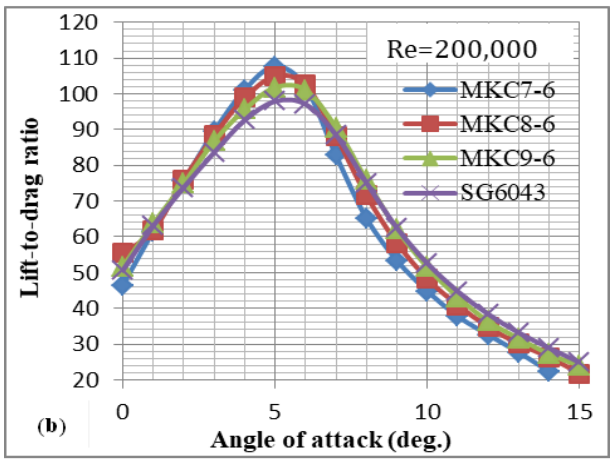

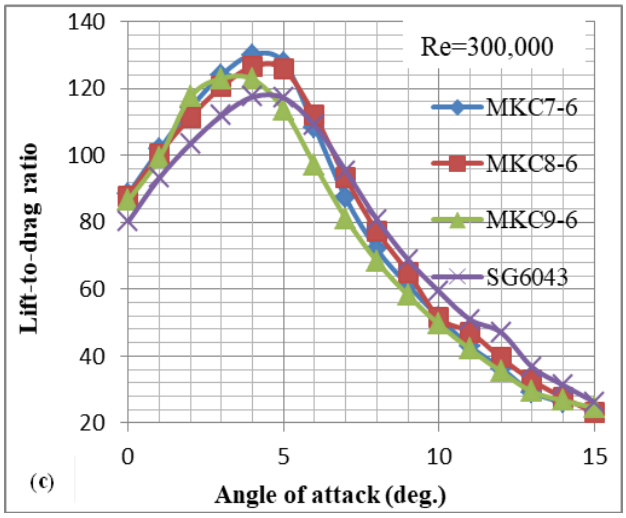

Fig. 15: Lift-to drag ratio versus AOA of SG6043 and MKC-Series airfoil (a) Re=100,000 (b) Re=100,000 (c) Re=300,000.

Figure 15 (a-c) shows the lift-drag ratio (L/D) performance of the NAF-Series airfoil and the basic airfoil at Re=100,000 to 300,000. Analytical results show that at Re=100,000, the maximum L/D ratios of the NAF 7-6, NAF 8-6, NAF9-6, and SG6043 airfoil are 71.16, 70.89, 68.9, and 66.6. Maximum L/D ratios at Re=200,000 for the MKC7-6, MKC8-6, MKC9-6, and SG6043 airfoil were 101.92, 104.9, 101.8, and 97.9, respectively, at AOAs of 4°, 5°, 5°, and 5°. The maximum L/D ratios for AOAs of 4°, 5°, 5°, and 5° for the NAF7-6, NAF8-6, NAF9-6, and SG6043 airfoil were 130.17, 125.8, 123.8, and 117.5 at Re=300,000, respectively. The results presented in Fig. 15 indicate that the NAF-Series airfoil outperforms the SG6043 in terms of L/D for Re between 100,000 and 300,000. In comparison to the SG6043 airfoil at Re=100,000 at an optimal AOA of 7°, the maximum L/D ratios of the MKC7-6, MKC8-6, and MKC9-6 airfoils are 6.98%, 6.05%, and 3.45%, respectively. Maximum L/D ratios of 3.94%, 6.66%, and 3.83% were observed for the NAF7-6, NAF8-6, and NAF9-6 airfoil, respectively, in comparison to the SG6043 airfoil at Re=200,000 at an optimal AOA of 4 to 5 degrees. The highest L/D ratios of the NAF7-6, NAF8-6, and NAF9-6 airfoil were 9.73%, 6.35%, and 5.08%, respectively, when compared to the SG6043 airfoil at Re=300,000 at a best AOA of 4 to 5 degrees accordingly. For the MKC7-6, MKC8-6, MKC9-6, and SG6043 airfoil, the ideal angles of attack were 4°, 5°, 5°, and 5°. At Re = 200,000, these values produced the highest L/D ratios of 101.92, 104.9, 101.8, and 97.9. The highest L/D ratios of 130.17, 125.8, 123.8, and 117.5 were achieved by the airfoil MKC7-6, MKC8-6, MKC9-6 and SG6043 at Re = 300,000.

4.3 Power coefficient performance of MKC-Series airfoil and MKC9-6 airfoil

For a 3-bladed, 0.4 m rotor diameter, power coefficient curves were generated for the best blade geometry. An experimented results of MKC-Series airfoil are presented in Fig. 16. (a) at Re=100, 000. Power performance curve of MKC9-6 airfoil for Re=100,000 to 300,000. The maximum C_P for rotor of MKC7-6, MKC8-6 and MKC9-6 airfoil were obtained 0.42, 0.425 and 0.435 at Re=100,000. The optimized TSR=4.5 at Re=100,000. The blades were fabricated by using MKC9-6 airfoil section for wind tunnel testing. From the results the maximum Cp obtained of MKC9-6 airfoil rotor is 0.42, 0.443 and 0.448 at Re=100,000 to 300,000 optimized at tip speed ratio (TSR)=4 to 5.

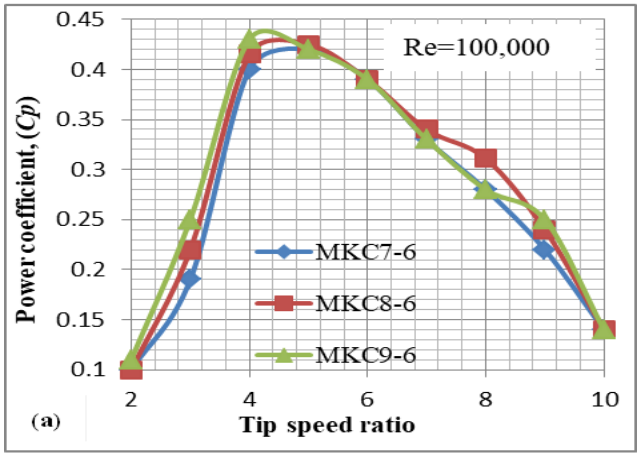

Fig. 16: Power coefficient versus TSR of new airfoil series at Re=100000.

4.4 Validation of the proposed airfoil with optimized airfoils of SWTs

The proposed airfoil was compared with the optimized SG6043 airfoil in this paper and SG6043 airfoil tested [11]. The proposed airfoil was tested with Re = 1×10^5 using X-Foil software for 2°–14° AOA with increments of 2°. For the X-Foil analysis, a turbulence intensity of 2% was selected because the conditions of the SG6043 airfoil test were approximately matched [11]. The graph of lift coefficient and lift–drag ratio distributions for SG6043 and NAF airfoils at Re = 1×10^5 at various AOA. The SG6043 and NAF airfoils exhibited a soft stall; the best behavior for small wind rotors at low Reynolds number. The NAF airfoil was 8% to 10% higher than the lift coefficient compared with SG6043 at AOA varying from 2° to 14°. L/D ratio for SG6043 and NAF airfoils for Re = 1×10^5. The L/D ratios produced by the NAF airfoil were 32, 63, 66, 56, 47, and 36 at the AOAs of 2°, 4°, 6°, 8°, 10°, and 12°, respectively. The L/D ratios produced by the SG6043 airfoil were 23, 37, 60, 62, 45, and 35 at the AOAs of 2°, 4°, 6°, 8°, 10°, and 12°, respectively by using XFoil. improving aerodynamic efficiency, the variations of normal forces along the 0.2 m blade length for the new airfoil and SG6043 airfoil. New airfoil shows good performance of normal forces along the length of the blade than an airfoil

4.5 Effect of pitch angle and tip speed ratio on rotor performance.

Numerical results were achieved using an XFoil and Numerical simulation under the exact same conditions as those of wind tunnel testing. Figure 17(a) depicts the experimentation results of variation in the rotor speed at various blade angle. Experimentations done at constant wind velocity of 8 m/s. Fig. 17(b) The results of numerical and experimental optimization are tabulated in Table 3. The validation results of numerical and experimental methods for the proposed airfoil rotors with a constant rated wind velocity of 8 m/s uncertainty results analysis as shown in Fig.16. The average error in the wind speed from2 to 10 m/s between numerical and experimental results was 10% to 12%.

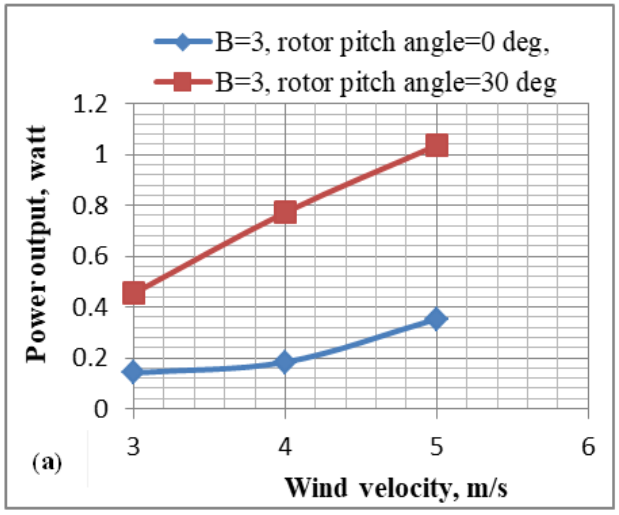

Fig. 17 (a): Rotor performance and Cp versus TSR for wind turbine rotor (a) MKC9-6 airfoil at Re=100,000 at Rotor pitch angle=0º & 30º.

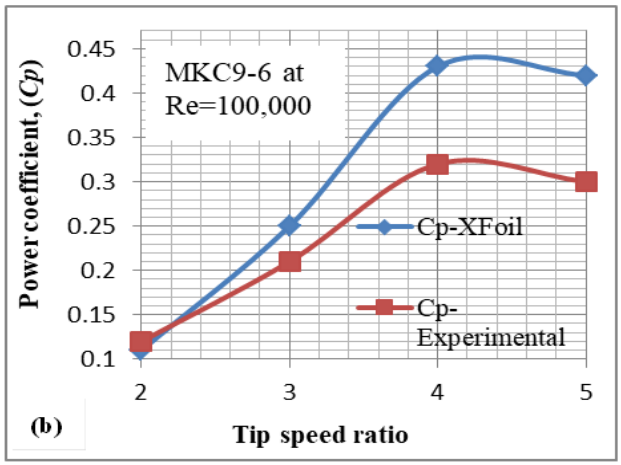

Fig. 17 (b): Rotor performance and Cp versus TSR for wind turbine rotor MKC9-6 airfoil at Re=100,000.

A 3-bladed rotor of the MKC9-6 airfoil at Re=100,000. Figure 17(a) shows the optimal electrical power plotted for the 0o and 30º pitch angles at various wind velocities. As can be observed, the rotor's power production is 0.45, 0.77, and 1.03 watts at optimal wind speeds (3 to 6 m/s) for rotor pitch angle = 30º, and 0.14, 0.183, and 0.35 watts at wind speeds of 3 to 5 m/s for rotor pitch angle = 0º. As the TSR (λ) increases, the Cp value first rises until it reaches 4.5 and then falls, as seen in Fig. 17. (b), at Re = 100,000, the optimized BEMT blades with the MKC9-6 airfoil had an experimental Cp of 0.32 at TSR (λ) = 4.5, compared to a theoretical Cp of 0.43. A rotor pitch angle of 30 degrees and a tip speed ratio of 4.5 are ideal. The aerodynamic performances of the MKC-Series airfoil rotor show good agreement with XFoil and wind tunnel test findings.

4.6 Experimental results and Uncertainty analysis

The numerical simulation so suggested that the NAF airfoil was the best airfoil to use when delivering the greatest power in low wind conditions. It has been established that good rotor efficiency is created in wind velocity ranges of 6 m/s to 10 m/s at Reynolds number varies from 100000 to 300000. When the blade is built with Reynolds number less than 100000, the shape of the airfoil directly affects the rotor performance and the tip speed ratio. According to the results of the experiment and theory, small horizontal axis wind turbines with low wind speeds are better suited for the rotor with airfoil MKC 9-6. Figure 18 displays the Rotor performances at different wind velocity. Up to a certain point, referred to as the rated speed, more electricity is produced as wind speeds rise is shows in Fig 18. The rated wind speed was fix at 10 m/s. Error propagation rates ranged from 80 to 85 percent recorded. According to the manufacturer catalogue, the highest tachometer accuracy was 0.785%. As a function of the rotor pitch and wind velocity variations, the power coefficient fluctuation is seen throughout. Use of this Reynolds number in small wind turbine rotors provides appropriate features because of its high power coefficient, maximum torque, and lower solidity (3% to 8%) at TSR 4 to 6. These factors help the rotor start up and run better at low wind velocities. In this work, a new blade shape and airfoil are created for small wind turbines operating at low wind speeds with low Re values. X-Foil and wind tunnel testing have addressed these analytical airfoil to forecast their aerodynamic performance for the anticipated operating numbers of Reynolds because they lack experimental drag, lift, and lift-drag ratio data. Airfoil with low drag coefficients and high lift-to-drag ratios were chosen from the anticipated results as potential rotor options for compact low-power wind turbines.

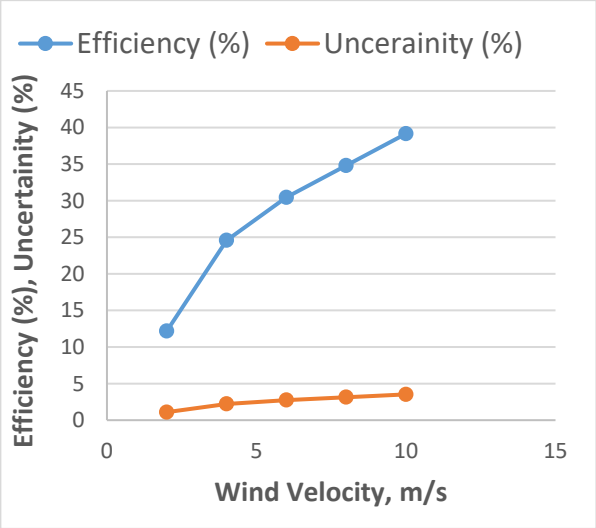

Fig. 18: Rotor performances at different wind velocity.

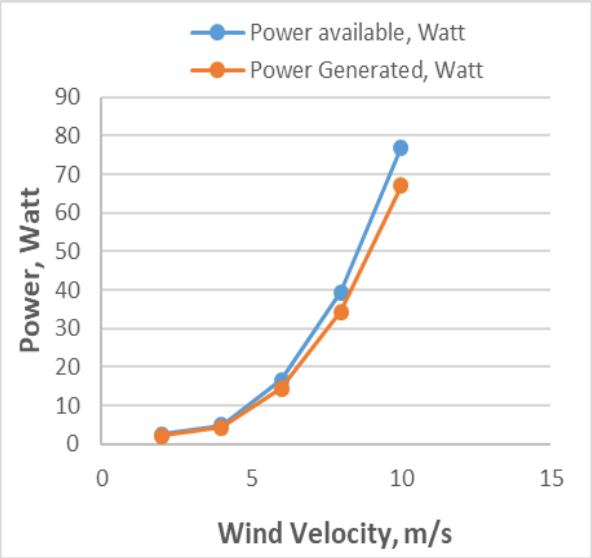

Fig. 19: Rotor Efficiency and Uncertainty analysis at different wind velocity.

The blade angle that was optimized was 35°. When the rotor radius or number of blades increased, the torque value also increased. As Fig. 19 illustrates, the uncertainty may be as low as 10%. This shows the degree of uncertainty in the wind speed as reported by the anemometers following data validation and adjustments. At the rated wind speed, the highest uncertainty resulted in 5%. At rated wind speed, the rotor's maximum efficiency is 40%. Estimates of wind resources are only useful if their degree of uncertainty is made explicit.

5. Conclusions

For small horizontal axis wind turbine rotor applications, three new airfoil (MKC-Series) were designed, produced, and tested in this work. The SG6043 basic airfoil was optimized and used to design the MKC (NAF)-Series airfoil using the thickness to camber ratio.

- The NAF-Series airfoil displayed high aerodynamic performance, with the highest combination of aerodynamic performances and the lowest drag coefficient value. In comparison to the SG6043 airfoil at Re=200,000 for the ideal AOA=4° to 5°, the MKC7-6, MKC8-6, and MKC9-6 airfoil had maximum L/D ratios of 3.94%, 6.66%, and 3.83%, respectively.
- The MKC9-6 had the highest stall angle of 14°, while MKC8-6 and MKC7-6 had maximum stall angle 13° and 12° respectively for Re=100,000. The MKC9-6 airfoil had the drag coefficient 0.021, 0.015, and 0.012 for Re=100,000 to 300,000 at AOA=6° Utilizing quick invention technique, a 3-bladed with a circular at the tip was optimized and designed for a 0.4 m rotor diameter.
- PLA was utilized in the design of the 3-blade rotor to make it lightweight and capable of operating at wind speeds ranging from 3 to 5 m/s. For the four possible pitch angles of 0 degree, 30 degrees, 45 degrees, and 90 degrees that were investigated in a wind tunnel, experimental results indicate that the optimal rotor pitch angle is 35 degrees. Regarding the MKC9-6 airfoil at Re=100,000 to 300,000 and TSR=4 to 5.

For Re=100,000 to 300,000, the three-bladed rotor with the MKC9-6 airfoil at TSR=4 to 5 produced theoretical Cp values of 0.42, 0.443, and 0.448. The MKC-series airfoil rotor achieved theoretical and practical Cp values of 0.43 and 0.32, respectively, at Re=100,000 at TSR=4.5. When a three-bladed rotor is used with a length blade of 0.2 meters and a rotor pitch angle of 30 degrees, its power production ranges from 2.5 to 70 watts at wind speeds of 3 to 10 m/s. The range of uncertainty is 1.5% to 4.5% between 12% and 40% of the rotor is efficient when the wind speed is between 3 and 10 m/s.

Acknowledgements

The authors would like to thank Trinity Academy of Engineering, Pune, India for providing the wind tunnel and FDM equipment.

Conflict of Interest

The authors declare no conflict of interest

Nomenclature

Re	Reynolds Number
TSR	Tip speed ratio
Cp	Power coefficient
AOA	Angle of attack (degree)
SG	Selig / Giguere Airfoil series.
MKC	New airfoil series (NAF 1-3).

References

1) Meng -Hsien Lee, Y. C. Shiah and Chi- Jeng Bai,"Experiments and numerical simulations of the rotor-blade performance for a small-scale horizontal axis wind turbine" *Journal of Wind Engineering an Industrial Aerodynamics, Elsevier*, pp. 17-29, (2016). http://dx.doi.org/10.1016/j.jweia.2015.12.002.
2) Ismail K. A. R., Canale T., and Lino F. A. M., "Parametric analysis of Joukowski airfoil for 10-kW horizontal axis windmill", *Journal of the Brazilian Society of Mechanical Sciences and Engineering,* Articleno.179, 40, (2018) https://doi.org/10.1007/s40430-018-1119-3.
3) Md. Abu Abrar, Ishtiaque A M Mahbub and Mohammad Mamun, "Design Optimization of A Horizontal Axis Micro Wind Turbine through Development of CFD Model And Experimentation" *Procedia Engineering, 10th International Conference on Mech. Engineering, ICME,* Vol. No. 90, pp.333-338,(2013),https://doi.org/10.1016/j.proeng.2014.11.858.
4) Wright A. K, Wood D. H., "The starting and low wind speed behaviour of a small horizontal axis wind turbine". *Journal of Wind Engineering and Industrial Aerodynamics,*92:12651279(2004). https://doi.org/10.1016/j.jweia.2004.08.003.
5) Clifton-Smith M. J, Wood D. H., "further dual purpose evolutionary optimization of small wind turbine blades". *J Phys. Conf. Ser., 2007;75:012017,* https://doi.org/10.1088/1742-6596/75/1/012017
6) Gur O, Rosen A., "Comparison between blade-element models of propellers". *Aeronaut J* ,112 (1138),pp.689–704,(2008) https://doi.org/10.13140/RG.2.1.3854.5129.
7) Hassanzadeh A., Hassanabad H. H, and Dadvand A., "Aerodynamic shape optimization and analysis of small wind turbine blades employing the Viterna approach for post-stall region", *Alexandria Engineering Journal,*;55(3),pp.2035-2043.(2016). https://doi.org/10.1016/j.aej.2016.07.008.
8) Saravanan, P., Parammasivam, K., and Rajan, S.,"Experimental Investigation on Small Horizontal Axis Wind Turbine Rotor Using Winglet'', *Journal of Applied Science andEngineering,*;Vol.16,No.2,pp.159-14.(2013). https://doi.org/10.6180/jase.2013.16.2.07.
9) Mohamed Khaled., Ibrahim M. M, Hamed A H, Ahmed F., "Investigation of a SHAWT turbine performance with and without winglet", *Energy,2019;* https://doi.org/187:115921.https://doi.org/10.1016/j.
10) Nataraj M. and Balaji G., "Study on performance of wind mill by adding winglet in turbine blade: Virtual analysis", *Journal of scientific &industrial research,* Vol. 78, pp. 96-101, (2019).
11) Suresh A. and S. Rajakumar, "Design of small horizontal axis wind turbine for low wind speed rural applications", *Materials today: Proceeding,*23(1),pp.16-22, (2019). https://doi.org/10.1016/j.matpr.2019.06.008.
12) Duquette, M. M. and Visser, K.D., "Numerical Implication of Solidity and Blade Number on Rotor Performance of Horizontal-Axis Wind Turbines", *Journal of Solar Energy Engineering*, Vol. No. 125,pp.425-432, (2003). https://doi.org/10.1115/1.1629751.
13) Singh RK, Ahmed M R, Zullah M A, Lee Y-H., "Design of a low Reynolds number airfoil for small horizontal axis wind turbines" *Renewable Energy, Elsevier,* Vol. 42, pp.66–76,(2012). https://doi.org/10.1016/j.renene.2011.09.014.
14) Giguere P, Selig MS. "New airfoil for small horizontal axis wind turbines".ASME *Journal of Solar Energy Engineering 1998*: 120:108-14
15) Ismail K. A. R and Celia V. A. G Rosolen, "Effects of the airfoil section, the chord and pitch distributions on the aerodynamic performance of the propeller", *Journal of the Brazilian Society of Mechanical Sciences and Engineering*,41:131,(2019). https://doi.org/10.1007/s40430-019-1618-x.
16)Sessarego Matias and Wood David, "Multi-dimensional optimization of small wind turbine blades",*Renewables Wind Water* and,Solar,Springer, 2,(9), (2015), https://doi.org/10.1186/s40807-015-000x
17) Husaru D. E., P D Barsanescu and D Zahariea, Effect of yaw angle on the global performances of Horizontal Axis Wind Turbine QBlade simulationI OPConf. Series: *Material Science andEngineering*;595,012047.(2019).https://doi.org/10.1088/1757-899X/595/1/01204.
18)Chaudhary, M.K. and Roy, A. (2015), "Design & optimization of a small wind turbine blade for operation at low wind speed", *World Journal of Engineering,*12(1)pp.83-94. https://doi.org/10.1260/17085284.12.1.83
19) Manoj Kumar Chaudhary and S. Prakash, "Optimizations of small horizontal-axis wind turbine rotors at low Reynolds number" , AIP ConferenceProceedings2311,030003(2020) https://doi.org/10.1063/5.0034319
20) Manoj Kumar Chaudhary and S. Prakash, Design and Fabrication of Small Horizontal axis wind Turbine Rotors at Low Reynolds Number, Technology and Exploring Engineering (IJITEE), 8(12),(2019). https://doi.org/10.35940/ijitee.L3499.1081219
21)Manoj Kumar Chaudhary and S. Prakash, "The Aerodynamic Shape Optimization for a Small Horizontal Axis Wind Turbine Blades at Low Reynolds Number*" Int. J. Mech. Prod. Eng. Res. Dev.,* 8 (6)pp. 843–854,(2018).
22) V. Singh, V. S. Yadav, R. Kumar and V. Trivedi,"Experimental and Numerical Analysis of Slurry Pot Tester by Response Surface Methodology (RSM) and Computational Fluid Dynamics (CFD),"

EVERGREEN Joint Journal of Novel Carbon Resource Sciences & Green Asia Strategy, vol. 10, no. 02,pp.931–941,(2023). https://doi.org/10.5109/6792888

23) Raed A. Jessam, "Experimental Study of Wind Turbine Power Generation Utilizing Discharged Air of Air Conditioner Blower" *EVERGREEN Joint Journal of Novel Carbon Resource Sciences & Green Asia Strategy,* 09(04),1103-1109, (2022). https://doi.org/10.5109/6625722.

24)M. Al-Ghriybah, "Assessment of wind energy potentiality at ajloun, jordan using weibull distribution function," *Evergreen*, 9 (1) 10–16(2022). https://doi.org/10.5109/4774211.1224422.

25) M.M. Takeyeldein, T.M. Lazim, N.A.R. Nik Mohd, I.S. Ishak, and E.A. Ali, "Wind turbine design using thin airfoil sd2030," *Evergreen*, 6 (2)114–123(2019). https://doi.org/10.5109/23210031255.

26)M.M. Takeyeldein, T.M. Lazim, I.S. Ishak, N.A.R. Nik Mohd, and E.A. Ali, "Wind lens performance investigation at low wind speed," *Evergreen,* 7 (4) 481–488 (2020). https://doi.org/10.5109/4150467.

27)M.Al-Ghriybah,"Performance Analysis of a Modified Savonius Rotor Using a Variable Blade Thickness." *Evergreen,* 9(3) 645–653 (2022). https://doi.org/10.5109/4842522

28)O.M.A.M. Ibrahim, and S. Yoshida, "Experimental and numerical studies of a horizontal axis wind turbine performance over a steep 2d hill," *Evergreen*, 5 (3) 12–21 (2018). https://doi.org/10.5109/1957496

29) A.M.M. Ismaiel, and S. Yoshida, "Study of turbulence intensity effect on the fatique lifetime of wind turbines," Evergreen, 5 (1), 25-32 (2018).https://doi.org/10.5109/1929727.

30)M.A.M. Ibrahim Omar, and Y. Shigeo, "Experimental and numerical studies of a horizontal axis wind turbine performance over a steep 2D hill," E*vergreen,* 5 (3), 12-21 (2018). https://doi.org/10.5109/1957496.

31) M.M. Takeyeldein, T.M. Lazim, N.A.R. Nik Mohd, I.S. Ishak, "Wind turbine design using thin airfoil SD2030"*Evergreen*,6(2),114-123(2019). https://doi.org/10.5109/2321003.